DTU Library

Protic ionic liquids with low viscosity for efficient and reversible capture of carbon dioxide

Li, Fangfang; Bai, Yinge; Zeng, Shaojuan; Liang, Xiaodong; Wang, Hui; Huo, Feng; Zhang, Xiangping

Protic ionic liquids with low viscosity for efficient and reversible capture of carbon dioxide

Fangfang Li[a,b], Yinge Bai[a], Shaojuan Zeng[a,**], Xiaodong Liang[c], Hui Wang[a], Feng Huo[a], Xiangping Zhang[a,b,*]

[a] Beijing Key Laboratory of Ionic Liquids Clean Process, CAS Key Laboratory of Green Process and Engineering, State Key Laboratory of Multiphase Complex Systems, Institute of Process Engineering, Chinese Academy of Sciences, Beijing 100190, China

[b] Sino-Danish College of University of Chinese Academy of Sciences, Beijing 100049, China

[c] Department of Chemical and Biochemical Engineering, Technical University of Denmark, DK-2800 Lyngby, Denmark

* Corresponding author. E-mail: xpzhang@ipe.ac.cn, Tel/Fex: 86-10-8254-4875

** Corresponding author. E-mail: sjzeng@ipe.ac.cn

Abstract

Protic ionic liquids (PILs) are considered as potential solvents for CO_2 capture due to their simple synthetic routes and unique properties. In this work, three low viscous PILs, tetramethylgunidinium imidazole ([TMGH][Im]), tetramethylgunidinium pyrrole ([TMGH][Pyrr]) and tetramethylgunidinium phenol ([TMGH][PhO]) were synthesized and the effect of anions, temperature, CO_2 partial pressure and water content on CO_2 absorption performance of PILs was also systematically studied. It was found that the PILs with larger basicity show higher CO_2 absorption capacity, and [TMGH][Im] simultaneously shows relatively high absorption rate and CO_2 absorption capacity of 0.154 g CO_2/g IL at 40 °C, 1 bar. The addition of H_2O has a positive effect on gravimetric absorption capacity of CO_2 at the range of 0-20 wt% H_2O, and the highest capacity of 0.186 g CO_2/g IL was achieved as the water content was 7 wt%. *In-situ* FTIR, ^{13}C NMR and theoretical calculations verified that more stable bicarbonate are produced during CO_2 absorption by [TMGH][Im]-H_2O system. However, neat [TMGH][Im] can react with CO_2 to form the reversible carbamate, leading to excellent recyclability after four absorption-desorption cycles. The results implied that neat [TMGH][Im] shows great potentials in CO_2 absorption applications.

Keywords: Ionic liquids, protic, low viscosity, CO_2 absorption, mechanisms

1. Introduction

Greenhouse effect caused by carbon dioxide (CO_2) emission has become one of the most serious environmental problems in the global area and awakened wide attention due to the excessive combustion of fossil fuels (Mondal et al., 2012). Therefore, developing new technologies to reduce CO_2 emission is the main concern (Guo et al., 2015; Ozturk, 2015; Lazarevic et al., 2017). One of the most promising methods to mitigate the impact of greenhouse gas for climate change and CO_2 utilization is developing carbon dioxide capture and storage technologies (CCS) (Deng, 2016). Alkanolamines (including monoethanolamine, diethanolamine and N-methyldiethanolamine) are the most commonly applied solvents for CO_2 capture in industries (Han et al., 2011). However, aqueous alkanolamines for CO_2 capture have some intrinsic drawbacks, such as corrosivity and degradation during the regeneration of solvents. Besides, large heat capacity of water and easy volatilization of alkanolamines result in high solvent loss and intensive energy consumption (Vaidya and Kenig, 2007). Accordingly, there is a pressing demand for seeking novel CO_2 capture solvents with favorable absorption performance, low solvent loss and energy consumption.

Ionic liquids (ILs) have emerged as potential solvents for gas separation (Zhang et al., 2013; Gao et al., 2015; Cao et al., 2017; Shang et al., 2017; Zhu et al., 2017) due to their outstanding properties, such as high thermal stability, low heat capacity, negligible vapor pressure and adjustable nature. ILs as CO_2 absorbents is one of the most effective alternatives to replace conventional aqueous alkanolamines solvents. Since Blanchard

et al. (1999) reported that CO_2 can dissolve in ILs, while ILs do not dissolve in CO_2, a large number of publications on CO_2 capture by ILs through physical interaction were reported (Palomar et al., 2011; Sistla and Khanna, 2011; Zhao et al., 2011; Ramdin et al., 2012). However, CO_2 absorption capacity in these ILs is only about 0.03 mol CO_2/mol IL under atmospheric pressure (Wang et al., 2011). In order to improve CO_2 absorption capacity in ILs, the chemisorption ILs were designed by introducing basic functional groups into ILs. Bates et al. (2002) proposed a new strategy for chemical absorption of CO_2 by amino-functionalized IL 1-propylamide-3-butylimidazolium tetrafluoroborate ([apbim][BF_4]), the absorption capacity of CO_2 in this IL is 0.074 g CO_2/g IL at room temperature and atmospheric pressure. Subsequently, there have been many reports on CO_2 absorption using amino-functionalized ILs, including amine-based and amino acid-based ILs (Hu et al., 2014; Lv et al., 2016; Huang et al., 2018). Riisager et al (2014). synthesized a series of amino acid-based ILs as CO_2 absorbents, and high CO_2 capacity of 0.13 g CO_2/g IL was measured for [N_{66614}][Lys] at ambient condition. Recently, an extremely high CO_2 capacity up to 0.25 g CO_2/g IL have been achieved by using tri-*n*-butylethylphosphonium succinimide ([P_{4442}][Suc]) (Huang et al., 2017). Nevertheless, the difficulty in chemisorbing ILs is the extremely high viscosity and complex synthetic routes of most task-specific ILs. For example, [P_{4442}][Suc] with a viscosity as high as 998 mPa·s at 20 ℃ should be prepared through anion-exchange and neutralization reaction. Consequently, developing novel task-specific ILs with high CO_2 absorption performance, simple synthetic routes and low viscosity are the main tasks for CO_2 capture.

Protic ionic liquids (PILs) can be easily obtained through a neutralization reaction of Brønsted acid and base. Recently, PILs have caught considerable attention in CO_2 capture fields due to their simpler synthetic routes and lower costs compared to most of aprotic ionic liquids (AILs) (Mumford et al., 2015; Xu, 2017; Oncsik et al., 2018). For example, Alcantara et al. (2018) studied the CO_2 absorption performance in four potential PILs which were synthetized through one-step neutralization of diethylamine/ethanolamines and butanoic acids. The results indicated that the PILs 2-hydroxyethylammonium butanoate ([2HEA][Bu]) and N-methyl-2-hydroxyethylammonium butanoate ([m-2HEA][Bu]) exhibited significant higher CO_2 solubility than most ILs ones analyzed. Tetramethylguanidine (TMG), as a common kind of superbase, has been widely reacted with proton donors and the obtained TMG-based PILs were frequently used in different fields (Reddy et al., 2015; Porwal et al., 2016; Singh et al., 2017). In recent years, TMG-based PILs were applied in acid gases absorption due to low viscosity, simple synthetic routes and excellent absorption performance (Jin et al., 2011; Meng et al., 2018). However, current research of TMG-based PILs mainly focused on sulfur dioxide (SO_2) absorption, rarely on CO_2 absorption. The efficiency of SO_2 absorption mainly related to the reaction of SO_2 with N-H group in $[TMGH]^+$ cation forming an N-S bond (Wu et al., 2004), while the reactivity of CO_2 and $[TMGH]^+$ cation is not valid because of the low acidity of CO_2 (Jessop et al., 2012). Recently, a novel method for CO_2 capture by tunable anion-functionalized PILs based on the single-site interaction between the CO_2 and electronegative nitrogen or oxygen atom was reported, it was shown that CO_2

absorption capacity can be easily tuned by the IL basicity (Wang et al., 2011). Therefore, anion-functionalized PILs with TMG as the proton acceptor combining with reactive hydrogen in azole or phenol is suitable for CO_2 absorption because of the strong basicity of TMG.

In this work, considering the significant role of IL basicity on CO_2 absorption (Wang et al., 2011), three basic PILs were designed and synthesized by neutralizing TMG with different weak proton donors, including imidazole (Im), pyrrole (Pyrr) and phenol (PhO) with different dissociation constant (pK_a). CO_2 absorption performance of these ILs, including the effect of anions, temperature, CO_2 partial pressure and water content on CO_2 absorption, as well as recyclability in the absence and presence of H_2O were systematically studied. The CO_2 absorption mechanisms of these systems were also investigated by *in-situ* FTIR, ^{13}C NMR analysis and theoretical calculations.

2. Experimental section

2.1. Materials

The materials TMG, Im and Pyrr were purchased from Aladdin Industrial Corporation. PhO was obtained from Xilong Scientific Limited. All the above chemical reagents were obtained in the analytical purity grade and used without further purification. CO_2 (>99.9% purity) and nitrogen (N_2, >99.9% purity) gases were supplied by Beijing Beiwen Gases Factory.

2.2. Synthesis and characterization of PILs

Three target basic PILs, tetramethylgunidinium imidazole [TMGH][Im],

tetramethylgunidinium pyrrole [TMGH][Pyrr] and tetramethylgunidinium phenol [TMGH][PhO] were prepared by direct neutralization of an appropriate TMG with different weak proton donors (Im, Pyrr and PhO) at room temperature and atmospheric pressure for 24 h (**Scheme 1**), and the synthetic procedures were similar to our previous work (Zhao et al., 2010, 2011). After that, all the ILs were dried in the vacuum oven at 60 °C for 40 h before use. The water contents in these ILs were measured by using Karl Fischer titration (Mettler Toledo Coulometric KF titrator C20), and all the water contents were below 320 ppm.
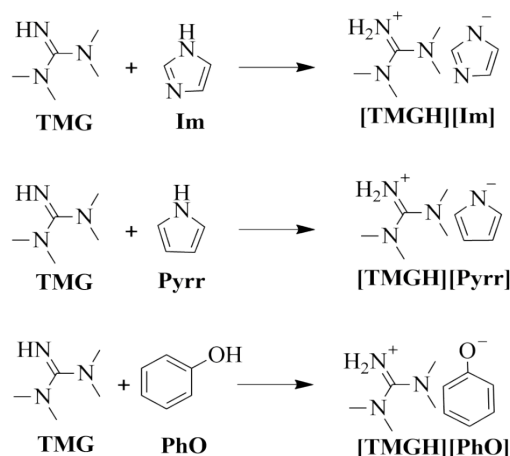
**Scheme 1**. Synthesis of [TMGH][Im], [TMGH][Pyrr] and [TMGH][PhO].

The obtained samples were characterized by ^{1}H and ^{13}C NMR using Bruker 600 spectormeter. FTIR spectra of these ILs were recorded in the range of 3600-400 cm^{-1} using Thermo Nicolet 380 spectrometer. Density and viscosity were measured using density meter (Anton Paar DMA 5000) and viscometer (Anton Paar AMVn) from 30 to 80 °C with 10 °C intervals under atmospheric pressure. The thermal stability of these ILs was measured using TGA Q5000 V3.15 with a heat rate of 10 °C/min in N$_2$ atmosphere at a flow rate of 20 ml/min. The ^{1}H NMR, ^{13}C NMR, FTIR spectra and

TGA data of all the studied PILs were concluded in the Supporting Information.

2.3. Absorption and desorption of CO_2

The experimental setup for CO_2 absorption is schematically represented in **Scheme 2**, and followed the procedures according to our previous work (Wang et al., 2014; Zeng et al., 2014, 2018). The absorption experiments were carried out in a glass container with an inner diameter of 2 cm. In a typical experiment, CO_2 gas (1) was bubbled through IL (about 5 g) in the glass container (9) at a flow rate of about 140 ml/min. The glass container was partly immersed in the water bath (8) at the desired temperature (the standard uncertainty of temperature is ± 0.1 ℃). The amount of absorbed CO_2 was determined at regular intervals by an electronic balance with an accuracy of ± 0.1 mg, which could remain constant when absorption of CO_2 reached to equilibrium. To ensure precision during weight measurements of samples, the glass container was dried outside before weighted.
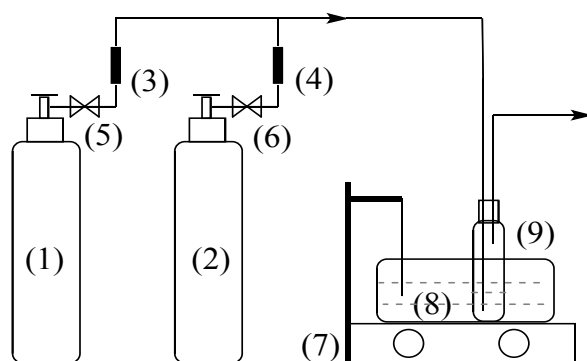
Scheme 2. Experimental diagram for CO_2 absorption. (1) CO_2 gas cylinder; (2) N_2 gas cylinder; (3) and (4) gas mass flowmeter; (5) and (6) valves; (7) magnetic stirrer; (8) water bath; (9) glass container with IL.

The effect of temperature on CO_2 absorption performance of ILs was carried out under atmospheric pressure by varying temperatures from 30 to 50 ℃. During CO_2 absorption under reduced pressure, the absorption temperature was kept constant at 40 ℃, the mixed gases with different CO_2 partial pressure were prepared by adjusting the flow rate of CO_2 and N_2 gases. To investigate the influence of water content on CO_2 absorption, CO_2 saturated with water vapor was bubbled through IL in the presence of different water content with 140 ml/min flow rate at 40 ℃ and atmospheric pressure.

For desorption process, CO_2-absorbed IL was transferred to a round-bottom flask and CO_2 was released by rotary evaporation at 60 ℃ for 2 h. The desorption of CO_2 from IL-H_2O system was similar to neat IL system, rotary evaporator was used to remove most of CO_2 and H_2O in CO_2 absorbed IL-H_2O system, the obtained product was dried in vacuum oven for 24 h to remove the residual moisture. Then fresh water was added to the obtained product at a certain ratio for next CO_2 absorption.

2.4 Computational methods

All calculations herein were performed with the Gaussian 09 program (Frisch et al., 2013) by using Density Functional Theory. All geometries of reactants, transition states and products were optimized at the M06-2X/def2-TZVP level of theory. The solvent effects of ILs were simulated by the SMD-GIL solvation model (Bernales et al., 2012). The frequency calculation was carried out at the same level to confirm the optimized structures to be energy minima without any imaginary frequency, and transition states has one and only one imaginary frequency. The interaction energies (or

energy barriers) were calculated as the energy difference between the products (or transition states) and the reactants.

3. Results and discussion

### 3.1. Physical properties of PILs

Physical properties, such as density and viscosity of ILs are important parameters for industrial application of CO_2 absorbents. Therefore, densities and viscosities of these PILs at various temperatures were measured and the results are shown in **Fig. 1** and **2**, respectively. The experimental density results for three ILs from 30 to 80 ℃ showed that temperature dependences of ILs densities have the linear behavior and decreased with the increasing of temperature. The density order of these ILs are: [TMGH][PhO] > [TMGH][Im] > [TMGH][Pyrr].

The viscosity of absorbents has significant effect on mass transfer during CO_2 absorption. ILs with low viscosities can result in low mass transfer resistance between liquid and gas phases, and thereby increase CO_2 absorption rate. As seen in **Fig. 2**, the viscosities of all studied ILs decreased with an increase in temperature. The viscosities of [TMGH][Im], [TMGH][Pyrr] and [TMGH][PhO] were 6.44, 2.10 and 26.77 mPa·s at 30 ℃, respectively, which are far lower than most of conventional ILs, for example, the viscosity of [Bmim][BF$_4$] was 68.90 mPa·s at 30 ℃ (Zhao et al., 2010). The results indicated that all these ILs have relatively low viscosities, which facilitate CO_2 diffusion in ILs during absorption processes.
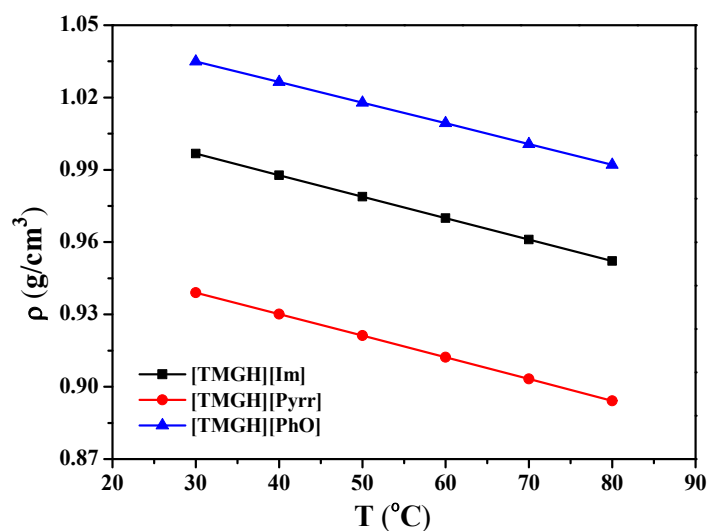
**Fig. 1.** Densities of [TMGH][Im], [TMGH][Pyrr] and [TMGH][PhO] at various
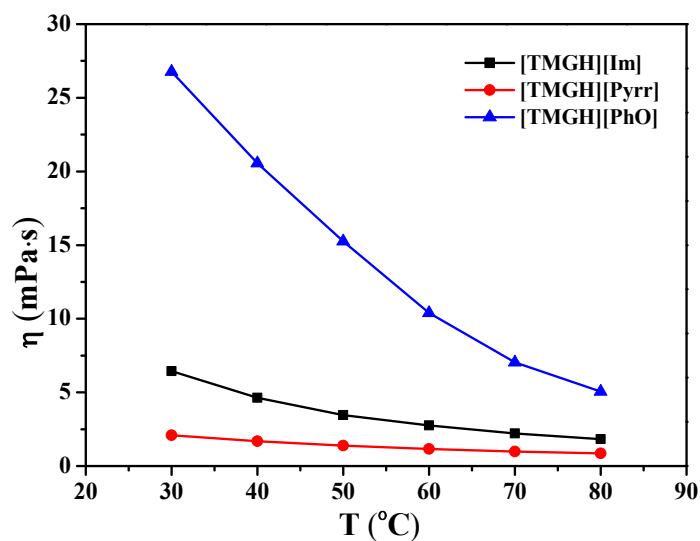
temperatures.

Fig. 2. Viscosities of [TMGH][Im], [TMGH][Pyrr] and [TMGH][PhO] at various

temperatures.

3.2. Effect of anions on CO_2 absorption

In order to investigate the CO_2 absorption performance in these PILs, CO_2 capture

experiments were firstly carried out in three PILs with different anions, [TMGH][Im],

[TMGH][Pyrr] and [TMGH][PhO] at 40 °C under atmospheric pressure in **Fig. 3**. It was

found that CO_2 absorption in all the ILs is very quick at the beginning, then decreased gradually and finally achieved equilibrium. Among the three ILs, [TMGH][Im] and [TMGH][Pyrr] exhibited higher CO_2 absorption capacity of 0.154 and 0.159 g CO_2/g IL, respectively, while CO_2 absorption capacity of [TMGH][PhO] was only 0.010 g CO_2/g IL at the same condition. In fact, CO_2 absorption capacity is significantly affected by the basicity of ILs. In general, the anion of ILs with larger pKa has higher CO_2 absorption capacity due to its stronger reactivity with CO_2 (Wang et al., 2011). As shown in **Table 1**, when the pKa of anions in DMSO decreased from 23.0 to 16.4, CO_2 molar absorption capacity decreased remarkably from 0.66 to 0.05 mol CO_2/mol IL.
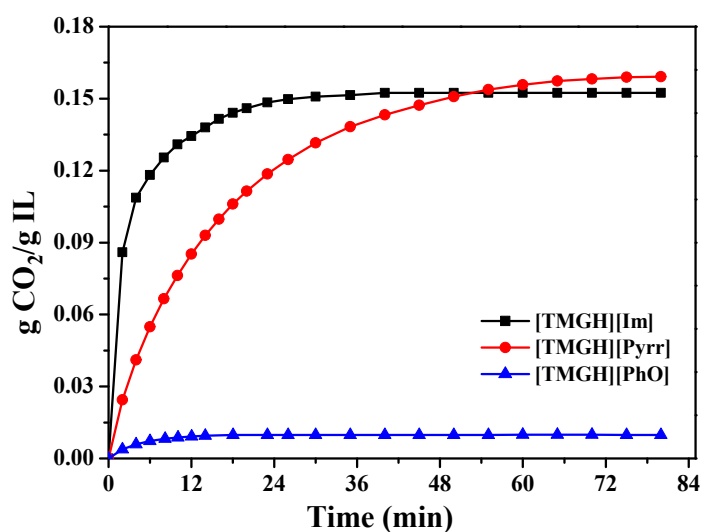
Fig. 3. CO_2 absorption in [TMGH][Im], [TMGH][Pyrr] and [TMGH][PhO] at 40 ℃ and 1 bar.

**Table 1**: The effect of anions pK_a on the CO_2 absorption capacity.

IL	M (g/mol)	T (°C)	Capacity (mol CO_2/mol IL)	pK_a in DMSO
[TMGH][Pyrr]	182.27	40	0.66	23.0 (Bordwell et al., 1981)
[TMGH][Im]	183.26	40	0.64	18.6 (Bordwell, 1988)
[TMGH][PhO]	209.29	40	0.05	16.4 (Ritchie, 1969)

Meanwhile, [TMGH][Im] also showed the faster rate of CO_2 absorption than other PILs, and the absorption can achieve equilibrium in 20 min. Although [TMGH][Pyrr] has the lowest viscosity, the absorption of CO_2 was completed in nearly 60 min, which is substantially three times that of [TMGH][Im]. The possible reason is that the solid state product was observed in [TMGH][Pyrr] after CO_2 absorption, which caused an increase in the apparent slurry viscosity, and reduction in effective diffusivity of CO_2 in the liquid (Kumar et al., 2003). As described above, [TMGH][Im] has a relative high CO_2 absorption capacity and the highest absorption rate compared with the other two ILs, which can be considered as a candidate solvent for CO_2 capture. Therefore, the effect of temperature, CO_2 partial pressure and water content on CO_2 absorption performance in [TMGH][Im] were further investigated and discussed.

3.3. Effect of temperature on CO_2 absorption

Temperature plays a key role in CO_2 absorption process, hence the effect of

temperature on CO_2 absorption performance of [TMGH][Im] was investigated from 30 to 50 ℃ under atmospheric pressure as shown in **Fig. 4**. The results indicated that CO_2 absorption capacity decreased obviously with temperature increasing. The absorption capacity of [TMGH][Im] was 0.177 g CO_2/g IL at 30 ℃, but reduced to 0.124 g CO_2/g IL at 50 ℃. This is because CO_2 absorption is an exothermic process, and the increasing of temperature is not favorable for CO_2 absorption. On the other hand, increasing temperature has a positive influence on mass transfer during the absorption of CO_2 due to lower viscosity of absorbents at higher temperature, and finally decreases saturation time. The saturation time decreased from 40 to 15 min when temperature changed from 30 to 50 ℃.
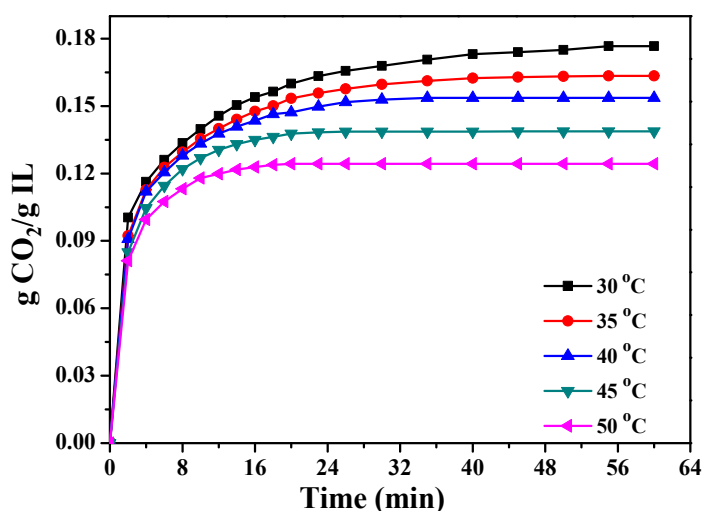
Fig. 4. CO_2 absorption in [TMGH][Im] at various temperatures.

3.4. Effect of partial pressure on CO_2 absorption

In industrial processes, CO_2 frequently coexists with other gases and CO_2 partial pressure almost lower than 1.0 bar. As illustrated in **Fig. 5**, CO_2 absorption performance of [TMGH][Im] was carried out at 40 ℃ with a CO_2 partial pressure of 0.1, 0.3, 0.5,

0.7, 0.9 and 1.0 bar to study the effect of CO_2 partial pressure on CO_2 absorption. With the decreasing of CO_2 partial pressure, CO_2 absorption capacity of [TMGH][Im] reduced gradually. The absorption capacity of [TMGH][Im] was as low as 0.05 g CO_2/g IL at 0.1 bar. From the investigation of the effect of temperature and CO_2 partial pressure on CO_2 absorption performance, both increasing CO_2 partial pressure and reducing temperature are benefit for enhancing CO_2 absorption capacity.
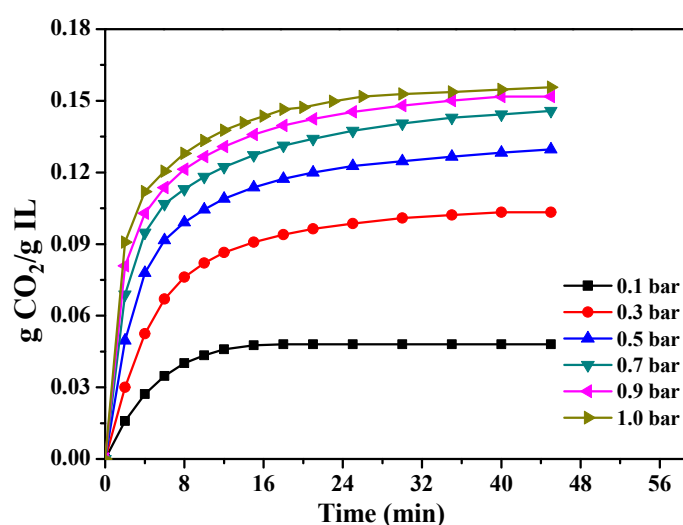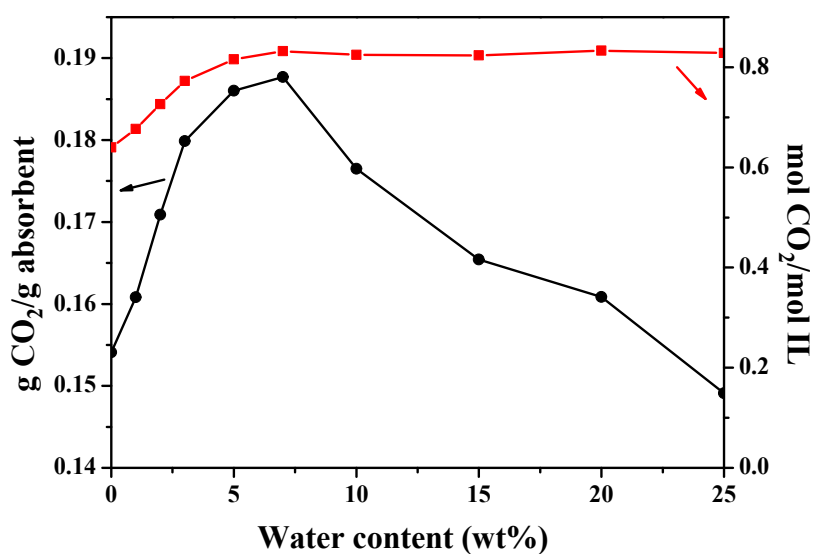

Fig. 5. CO_2 absorption in [TMGH][Im] at various CO_2 partial pressures.

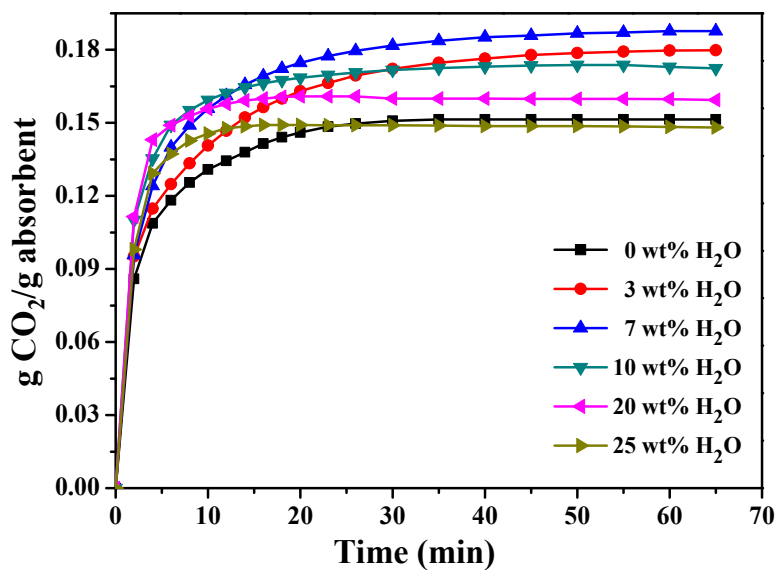## 3.5. Effect of water content on CO_2 absorption

The effect of water content on CO_2 absorption performance of [TMGH][Im] was also investigated under 40 °C and atmospheric pressure. As seen in **Fig. 6** and **7**, water contents can remarkably affect the CO_2 capacity of [TMGH][Im]. At the beginning, both CO_2 gravimetric and molar absorption capacity increased greatly with the increasing of water content, the highest absorption capacity up to 0.186 g CO_2/g absorbent (0.83 mol CO_2/mol IL) when 7 wt% H_2O was added to [TMGH][Im]. CO_2 gravimetric absorption capacity of absorbents reduced with an increase of water content

15

but still higher than that in neat [TMGH][Im] in the range from 7 to 20 wt% H_2O, which

was 0.161 g CO_2/g absorbent in 80 wt% [TMGH][Im]-20 wt% H_2O system, but CO_2

molar absorption capacity was almost maintain at 0.83 mol CO_2/mol IL. The possible

reason is that CO_2 can directly react with the imidazole anion to form the carbamate

product in neat [TMGH][Im], while in the presence of H_2O, the imidazole anion

interacts more strongly with the H_2O than CO_2, and a more stable bicarbonate and

neutral Im may generate after absorption of CO_2, resulting in an increase in CO_2

absorption capacity (Thompson et al., 2014). On the contrary, excessive quantities of

H_2O have a negative influence on CO_2 gravimetric absorption capacity of

[TMGH][Im]-H_2O systems due to the reducing of [TMGH][Im] content, it is also

shown that CO_2 gravimetric absorption capacity becomes lower when 25 wt% H_2O was

existed in [TMGH][Im], which was 0.149 g CO_2/g absorbent. The detail reason will be

discussed in the section of absorption mechanism.

Fig. 6. CO_2 absorption capacity of [TMGH][Im]-H_2O systems at 40 ℃ and 1 bar.

Fig. 7. Effect of water content on CO_2 absorption performance of [TMGH][Im] at

40 ℃ and 1 bar.

3.6. CO$_2$ absorption mechanisms in PILs

As aforementioned, the addition of H_2O changed the CO_2 absorption performance

of [TMGH][Im]. In order to understand the absorption mechanism of [TMGH][Im] in

the absence and presence of H_2O, *in-situ* FTIR, ^{13}C NMR and theoretical calculations

were used to analyze the interaction between ILs or IL-H_2O system and CO_2.

3.6.1 In-situ FTIR and NMR analysis

The [TMGH][Im]-H_2O system containing 80 wt% [TMGH][Im] and 20 wt% H_2O

showed higher absorption capacity and faster absorption rate. Therefore, neat

[TMGH][Im] and 80 wt% [TMGH][Im]-20 wt% H_2O system were selected to

investigate the absorption mechanism of [TMGH][Im] in the absence and presence of

H_2O via *in-situ* FTIR and ^{13}C NMR spectra. As shown in **Fig. 8**, the FTIR spectra of

the CO_2-absorbed [TMGH][Im] contained three new peaks compared to neat [TMGH][Im]. The peaks at 1700 and 1293.7 cm^{-1} can be attributed to the stretching vibrations of C=O and C-O of carbamate, respectively. The peak at 1176.3 cm^{-1} was appeared due to the formation of C-N. The results indicated that the carbamate was formed between the basic nitrogen of imidazole anion and CO_2 (Wang et al., 2011; Zhu et al., 2017). For [TMGH][Im]-H_2O system, two new characteristic peaks at 1252.7 and 1040.2 cm^{-1} appeared as shown in **Fig. 9** verified the formation of the bicarbonate during the absorption of CO_2, which means that new product was generated in the presence of H_2O. Furthermore, By analyzing ^{13}C NMR of [TMGH][Im]-based solvents before and after absorption of CO_2 listed in **Fig. 10**, a new carbon signal at 161.16 was observed in the CO_2-absorbed [TMGH][Im] as compared to neat [TMGH][Im], which was attributed to carbonate carbonyl carbon, while the peak at 160.26 ppm appeared after CO_2 absorption in [TMGH][Im]-H_2O was due to the formation of bicarbonate. (Andrews et al., 2011; Simon et al., 2017; Chen et al., 2018). The results were in agreement with relevant researches reported in literature that the basicity of anion can activate the reaction between CO_2 and H_2O to form conjugate acid of the basic anion and bicarbonate (Huang et al., 2019). Based on the above analysis, the possible CO_2 absorption mechanism of [TMGH][Im] in the absence and presence of H_2O was proposed in **Scheme 3**.
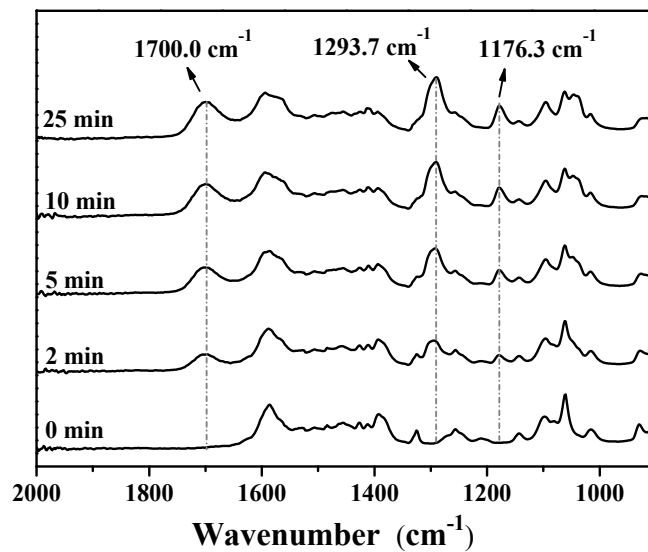
Fig. 8. FTIR spectra of [TMGH][Im] before and after absorption of CO_2.
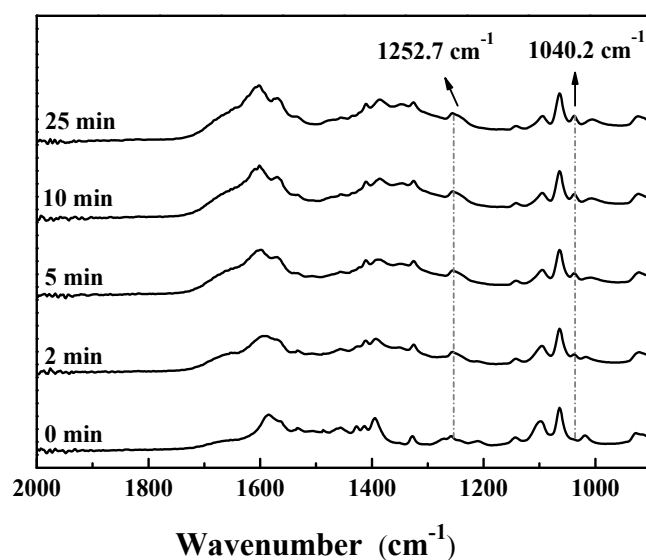

Fig. 9. FTIR spectra of [TMGH][Im]-H_2O system before and after absorption of CO_2.
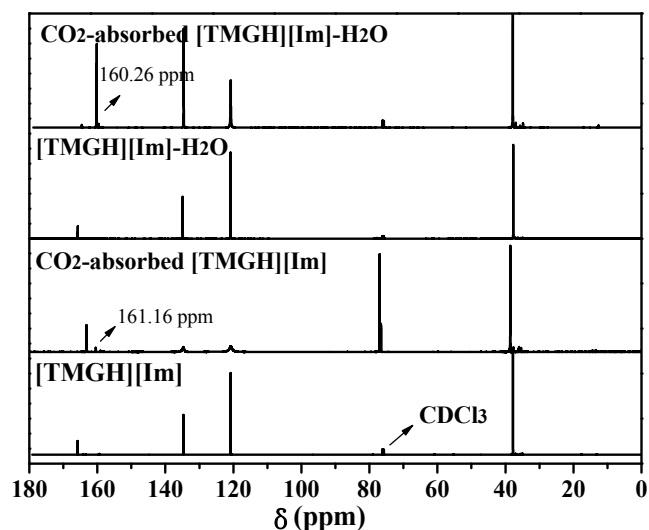
Fig. 10. ^{13}C NMR spectra of [TMGH][Im] and [TMGH][Im]-H_2O systems before and

after absorption of CO_2.

3.6.2 Quantum chemistry calculations

Based on the above experimental results and spectral characterizations, we proposed the possible CO_2 absorption pathways of [TMGH][Im] in the absence (pathway 1) and presence (pathway 2) of H_2O in **Scheme 3**. During the absorption of CO_2 in [TMGH][Im], carbamate (P1) is generated from the combination of nitrogen atom of N1 on the imidazole anion and CO_2 through transition states (TS1). When H_2O is existed in [TMGH][Im], the formation of N1-H4 and C2-O3 bonds generates the bicarbonate (P2) and Im via the transition states (TS2).

20
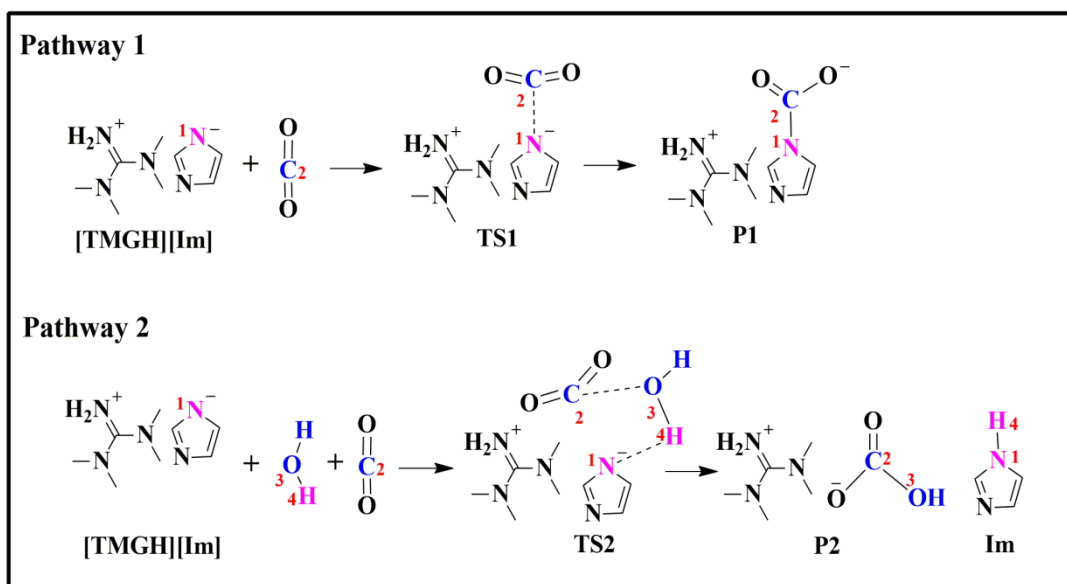
**Scheme 3**. CO_2 absorption pathways of [TMGH][Im] and [TMGH][Im]-H_2O systems

The CO_2 reaction potential energies for two systems are shown in **Fig. 11**. It can be seen that the reaction energy barriers of CO_2 with [TMGH][Im] and [TMGH][Im]-H_2O were 4.45 and 5.61 kcal/mol, respectively. The low energy barriers make CO_2 absorption easy to perform both in neat [TMGH][Im] and [TMGH][Im]-H_2O systems. The interaction energies of products P1 and P2 + Im were -12.26 and -14.86 kcal/mol, respectively. These data suggested that more stable bicarbonate was generated in the presence of H_2O, which is in good agreement with the experimental results.
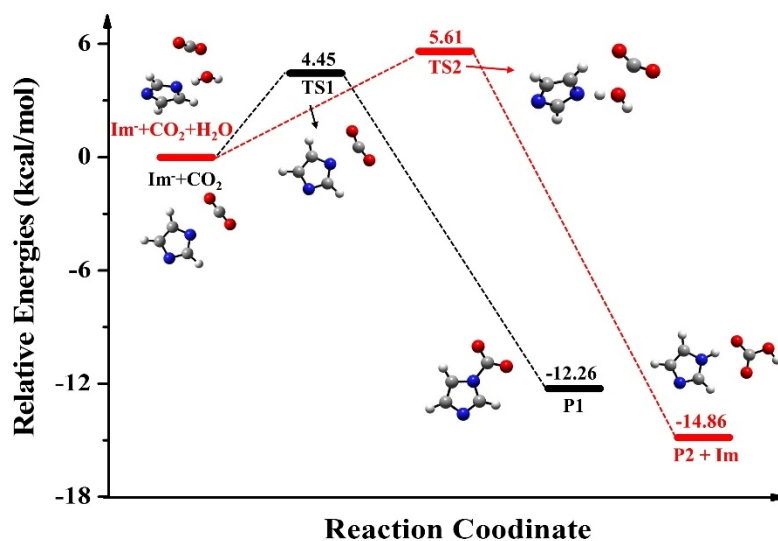
Fig. 11. Optimized structures and potential energy profiles of CO_2 absorption in [TMGH][Im] and [TMGH][Im]-H_2O systems

3.7. Recycle of [TMGH][Im] systems

In order to examine the recyclability of [TMGH][Im] systems, CO_2-absorbed IL systems were regenerated and reused for CO_2 absorption. As illustrated in **Fig. 12**, four absorption-desorption experiments by [TMGH][Im] showed that [TMGH][Im] can be repeatedly recycled without obvious loss of CO_2 absorption capacity. The results indicated that [TMGH][Im] as a novel CO_2 absorbent has an excellent performance for the reutilization and effective CO_2 absorption-desorption ability.

22
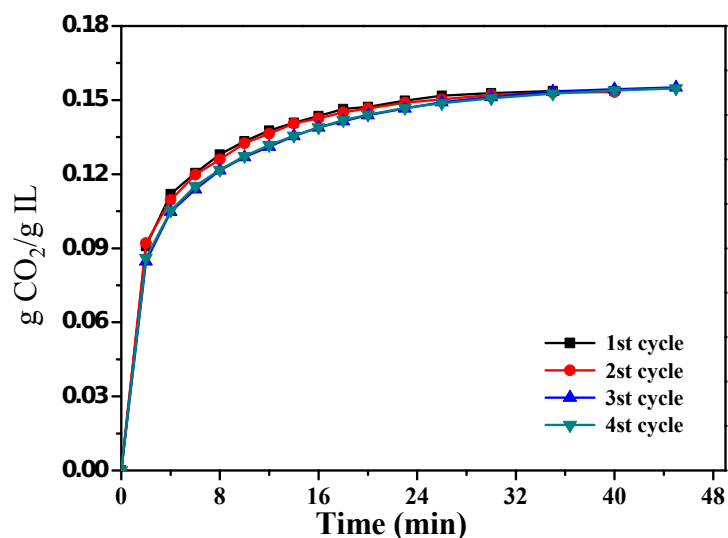
Fig. 12. Recycling of [TMGH][Im] for CO_2 absorption at 40 ℃ and 1 bar.

For the system of 80 wt% [TMGH][Im]-20 wt% H_2O, CO_2 absorption capacity obviously decreased with the increasing of recycle times as demonstrated in **Fig. 13**. Such solvent is not suitable for industrial CO_2 capture even it has high CO_2 capacity in the first cycle. As seen in **Fig. 11**, energy barriers for the desorption of CO_2 from carbamate and bicarbonate + Im systems were 16.71 and 20.47 kcal/mol, separately. The higher energy barrier makes it difficult to strip CO_2 from bicarbonate and Im.
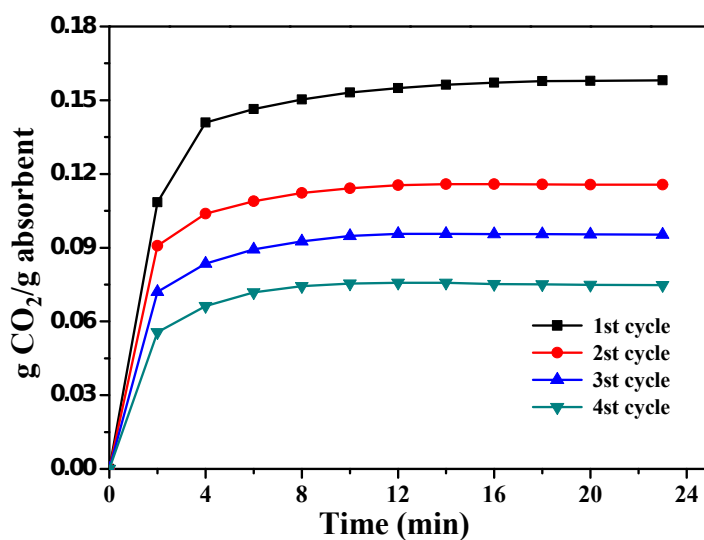
Fig. 13. Recycling of [TMGH][Im]-H_2O system for CO_2 absorption at 40 ℃ and 1 bar.

4. Conclusions

In summary, three low viscous PILs with different basicity were designed and synthesized by one-step route for efficient absorption of CO_2. The viscosity of [TMGH][Im], [TMGH][Pyrr] and [TMGH][PhO] were 6.44, 2.10 and 26.77 mPa·s at 30 ℃, separately, which is quite low compared with conventional ILs. The relationships between the basicity of ILs and their absorption performance of CO_2 indicated that ILs with larger pKa of anions has higher CO_2 absorption capacity. The addition of H_2O changed CO_2 absorption performance of [TMGH][Im], gravimetric absorption capacity of CO_2 firstly increased and then decreased gradually with water content, the highest absorption capacity of 0.186 g CO_2/g absorbent (0.83 mol CO_2/mol IL) at 40 ℃ and 1 bar was obtained in 93 wt% [TMGH][Im]-7 wt% H_2O system. *In-situ* FTIR, ^{13}C NMR and theoretical calculations confirmed that carbamate can be formed reversibly during the absorption of CO_2 in [TMGH][Im], the good recyclability after four absorption-desorption cycles indicating that [TMGH][Im] as a potential alternative for CO_2 capture has an excellent performance for the effective CO_2 absorption-desorption ability. The existence of H_2O result in larger energy barrier during the desorption of CO_2, so it is necessary to make sure that water content in [TMGH][Im] is quite low to ensure excellent recyclability of [TMGH][Im] in CO_2 capture application.

Acknowledgment

Reference

Alcantara, M.L., de Carvalho, M.L., Alvarez, V.H., Ferreira, P.I.S., Paredes, M.L.L., Cardozo, L., Silva, A.K., Liao, L.M., Pires, C.A.M., Mattedi, S., 2018. High pressure vapor-liquid equilibria for binary carbon dioxide and protic ionic liquid based on ethanolamines plus butanoic acid. Fluid Phase Equilib. 460, 162-174.

Alcantara, M.L., Santos, J.P., Loreno, M., Ferreira, P.I.S., Paredes, M.L.L., Cardozo, L., Silva, A.K., Liao, L.M., Pires, C.A.M., Mattedi, S., 2018. Low viscosity protic ionic liquid for CO_2/CH_4 separation: Thermophysical and high-pressure phase equilibria for diethylammonium butanoate. Fluid Phase Equilib. 459, 30-43.

Andrews, N.J., Haynes, C.J.E., Light, M.E., Moore, S.J., Tong, C.C., Davis, J.T., Harrell, W.A., Jr., Gale, P.A., 2011. Structurally simple lipid bilayer transport agents for chloride and bicarbonate. Chem. Sci. 2(2), 256-260.

Bates, E.D., Mayton, R.D., Ntai, I., Davis, J.H., 2002. CO_2 capture by a task-specific ionic liquid. J. Am. Chem. Soc. 124(6), 926-927.

Bernales, V.S., Marenich, A.V., Contreras, R., Cramer, C.J.,Truhlar, D.G., 2012. Quantum mechanical continuum solvation models for ionic liquids. J. Phys. Chem. B 116(30), 9122-9129.

Blanchard, L.A., Hancu, D., Beckman, E.J.,Brennecke, J.F., 1999. Green processing using ionic liquids and CO_2. Nature 399(6731), 28-29.

Bordwell, F.G., 1988. Equilibrium acidities in dimethyl-sulfoxide solution. Accounts Chem. Res. 21(12), 456-463.

Bordwell, F.G., Drucker, G.E., Fried, H.E., 1981. Acidities of carbon and nitrogen acids-the aromaticity of the cyclopentadienyl anion. J. Org. Chem. 46(3), 632-635.

Cao, L.D., Gao, J.B., Zeng, S.J., Dong, H.F., Gao, H.S., Zhang, X.P., Huang, J.H., 2017. Feasible ionic liquid-amine hybrid solvents for carbon dioxide capture. Int. J. Greenh. Gas Con. 66, 120-128.

Chen, C.-H., Shimon, D., Lee, J.J., Mentink-Vigier, F., Hung, I., Sievers, C., Jones, C.W., Hayes, S.E., 2018. The "missing" bicarbonate in CO_2 chemisorption reactions on solid amine sorbents. J. Am. Chem. Soc. 140(28), 8648-8651.

Deng, L.Y., 2016. CO_2 capture: challenge and opportunities. Green Energy & Environment 1(3), 179.

Frisch, M.J., Trucks, G.W., Schlegel, H.B., Scuseria, G.E., Robb, M.A., Cheeseman, J.R., Scalmani, G, Barone, V, Mennucci, B, Petersson, G.A., Nakatsuji, H., Caricato, M., Li, X., Hratchian, H.P., Izmaylov, A.F., Bloino, J., Zheng, G., Sonnenberg, J.L., Hada, M., Ehara, M., Toyota, K., Fukuda, R., Hasegawa, J., Ishida, M., Nakajima, T., Honda, Y., Kitao, O., Nakai, H., Vreven, T., Peralta, J.E., Ogliaro, F., Bearpark, M., Heyd, J.J., Brothers, E., Kudin, K.N., Staroverov, V.N., Keith, T., Kobayashi, R., Normand, J., Raghavachari, K., Rendell, A., Burant, J.C., Iyengar, S.S., Tomasi, M.C., Rega, J.M.M., Klene, M., Knox, J.E., Cross, J.B., Bakken, C.A., Jaramillo, Gomperts, R., Stratmann, O.Y., Austin, R., Cammi, C.P., Ochterski, R.L.M., Morokuma, V.G.Z., Voth, G.A., P Salvador, J.J.D., Dapprich, S., Daniels, A.D.,

Farkas, O., Foresman, J.B., Ortiz, J.V., Cioslowski, J., Fox, D.J., 2013. Gaussian 09, revision D.01, in, Gaussian, Inc., Wallingford CT.

Gao, J.B., Cao, L.D., Dong, H.F., Zhang, X.P.,Zhang, S.J., 2015. Ionic liquids tailored amine aqueous solution for pre-combustion CO_2 capture: Role of imidazolium-based ionic liquids. Appl. Energ. 154, 771-780.

Guo, Z., Liu, P., Ma, L.W., Li, Z., 2015. Effects of Low-carbon technologies and end-use electrification on energy-related greenhouse gases mitigation in China by 2050. Energies 8(7), 7161-7184.

Han, B., Zhou, C.G., Wu, J.P., Tempel, D.J., Cheng, H.S., 2011. Understanding CO_2 capture mechanisms in aqueous monoethanolamine via first principles simulations. J. Phys. Chem. Lett. 2(6), 522-526.

Hu, H., Li, F., Xia, Q., Li, X.D., Liao, L., Fan, M.H., 2014. Research on influencing factors and mechanism of CO_2 absorption by poly-amino-based ionic liquids. Int. J. Greenh. Gas Con. 31, 33-40.

Huang, Q.S., Jing, G.H., Zhou, X.B., Lv, B.H., Zhou, Z.M., 2018. A novel biphasic solvent of amino-functionalized ionic liquid for CO_2 capture: High efficiency and regenerability. J. CO_2 Util. 25, 22-30.

Huang, Y.J., Cui, G.K., Zhao, Y.L., Wang, H.Y., Li, Z.Y., Dai, S.,Wang, J.J., 2017. Preorganization and cooperation for highly efficient and reversible capture of low-concentration CO_2 by ionic liquids. Angew. Chem. Int. Edit. 56(43), 13293-13297.

Huang, Y.J., Cui, G.K., Zhao, Y.L., Wang, H.Y., Li, Z.Y., Dai, S.,Wang, J.J., 2019. Reply to the correspondence on "Preorganization and cooperation for highly

efficient and reversible capture of low-concentration CO_2 by ionic liquids". Angew. Chem. Int. Edit. 58, 386-389.

Jessop, P.G., Mercer, S.M.,Heldebrant, D.J., 2012. CO_2-triggered switchable solvents, surfactants, and other materials. Energ. Environ. Sci. 5(6), 7240-7253.

Jin, M.J., Hou, Y.C., Wu, W.Z., Ren, S.H., Tian, S.D., Xiao, L.,Lei, Z.G., 2011. Solubilities and thermodynamic properties of SO_2 in Ionic Liquids. J. Phys. Chem. B 115(20), 6585-6591.

Kumar, P.S., Hogendoorn, J.A., Feron, P.H.M.,Versteeg, G.F., 2003. Equilibrium solubility of CO_2 in aqueous potassium taurate solutions: Part 1. Crystallization in carbon dioxide loaded aqueous salt solutions of amino acids. Ind. Eng. Chem. Res. 42(12), 2832-2840.

Lazarevic, A., Karamarkovic, V., Lazarevic, D., Karamarkovic, R., 2017. Potentials and opportunities to reduce energy-related greenhouse gas emissions in Serbia. Energy Sources Part A-Recovery Util. Environ. Eff. 39(7), 712-719.

Lv, B.H., Xia, Y.F., Shi, Y., Liu, N., Li, W.,Li, S.J., 2016. A novel hydrophilic amino acid ionic liquid C(2)OHmim Gly as aqueous sorbent for CO_2 capture. Int. J. Greenh. Gas Con. 46, 1-6.

Meng, X.C., Wang, J.Y., Xie, P.T., Jiang, H.C., Hu, Y.Q.,Chang, T., 2018. Structure and SO_2 absorption properties of Guanidinium-based dicarboxylic acid ionic liquids. Energ. Fuel 32(2), 1956-1962.

Mondal, M.K., Balsora, H.K.,Varshney, P., 2012. Progress and trends in CO_2 capture/separation technologies: A review. Energy 46(1), 431-441.

28

Mumford, K.A., Pas, S.J., Linseisen, T., Statham, T.M., Nicholas, N.J., Lee, A., Kezia, K., Vijayraghavan, R., MacFarlane, D.R.,Stevens, G.W., 2015. Evaluation of the protic ionic liquid, N,N-dimethyl-aminoethylammonium formate for CO_2 capture. Int. J. Greenh. Gas Con. 32, 129-134.

Oncsik, T., Vijayaraghavan, R., MacFarlane, D.R., 2018. High CO_2 absorption by diamino protic ionic liquids using azolide anions. Chem. Commun. 54(17), 2106-2109.

Ozturk, I., 2015. Measuring the impact of energy consumption and air quality indicators on climate change: evidence from the panel of UNFCC classified countries. Environ. Sci. Pollut. Res. 22(20), 15459-15468.

Palomar, J., Gonzalez-Miquel, M., Polo, A.,Rodriguez, F., 2011. Understanding the physical absorption of CO_2 in ionic liquids using the COSMO-RS method. Ind. Eng. Chem. Res. 50(6), 3452-3463.

Porwal, J., Kumar, S., Kaul, S., Jain, S.L., 2016. Guanidine based task specific ionic liquids for the synthesis of biolubricant range esters under solvent-free condition. RSC Adv. 6(96), 93640-93644.

Ramdin, M., de Loos, T.W., Vlugt, T.J.H., 2012. State-of-the-art of CO_2 capture with ionic liquids. Ind. Eng. Chem. Res. 51(24), 8149-8177.

Reddy, M.V., Valasani, K.R., Lim, K.T., Jeong, Y.T., 2015. Tetramethylguanidinium chlorosulfonate ionic liquid (TMG IL): an efficient reusable catalyst for the synthesis of tetrahydro-1H-benzo a -chromeno 2,3-c phenazin-1-ones under solvent-free conditions and evaluation for their in vitro bioassay activity. New J.

Chem. 39(12), 9931-9941.

Ritchie, C.D., 1969. Proton transfer in dipolar aprotic solvents .V. solvation and geometric factors in rates of proton transfer reactions. J. Am. Chem. Soc. 91(24), 6749-6753.

Saravanamurugan, S., Kunov-Kruse, A.J., Fehrmann, R., Riisager, A., 2014. Amine-functionalized amino acid- based ionic liquids as efficient and high- capacity absorbents for CO_2. Chemsuschem 7(3), 897-902.

Shang, D.W., Zhang, X.P., Zeng, S.J., Jiang, K., Gao, H.S., Dong, H.F., Yang, Q.Y., Zhang, S.J., 2017. Protic ionic liquid Bim NTf_2 with strong hydrogen bond donating ability for highly efficient ammonia absorption. Green. Chem. 19(4), 937-945.

Simon, N.M., Zanatta, M., dos Santos, F.P., Corvo, M.C., Cabrita, E.J.,Dupont, J., 2017. Carbon dioxide capture by aqueous ionic liquid solutions. Chemsuschem 10(24), 4927-4933.

Singh, A.P., Sithambaram, D., Sanghavi, R., Gupta, P.K., Verma, R.S., Doble, M., Gardas, R.L., Senapati, S., 2017. Environmentally benign tetramethylguanidinium cation based ionic liquids. New J. Chem. 41(20), 12268-12277.

Sistla, Y.S., Khanna, A., 2011. Validation and prediction of the temperature-dependent Henry's constant for CO_2-ionic liquid systems using the conductor-like screening model for realistic solvation (COSMO-RS). J. Chem. Eng. Data 56(11), 4045-4060.

Thompson, R.L., Shi, W., Albenze, E., Kusuma, V.A., Hopkinson, D., Damodaran, K., Lee, A.S., Kitchin, J.R., Luebke, D.R.,Nulwala, H., 2014. Probing the effect of electron donation on CO_2 absorbing 1,2,3-triazolide ionic liquids. RSC Adv. 4(25),

12748-12755.

Vaidya, P.D.,Kenig, E.Y., 2007. CO_2-alkanolamine reaction kinetics: A review of recent studies. Chem. Eng. Technol. 30(11), 1467-1474.

Wang, C.M., Luo, X.Y., Luo, H.M., Jiang, D.E., Li, H.R.,Dai, S., 2011. Tuning the basicity of ionic liquids for equimolar CO_2 capture. Angew. Chem. Int. Edit. 50(21), 4918-4922.

Wang, J., Zeng, S.J., Bai, L., Gao, H.S., Zhang, X.P., Zhang, S.J., 2014. Novel ether-functionalized pyridinium chloride ionic liquids for efficient SO_2 capture. Ind. Eng. Chem. Res. 53(43), 16832-16839.

Wu, W.Z., Han, B.X., Gao, H.X., Liu, Z.M., Jiang, T., Huang, J., 2004. Desulfurization of flue gas: SO_2 absorption by an ionic liquid. Angew. Chem. Int. Edit. 43(18), 2415-2417.

Xu, Y.J., 2017. CO_2 absorption behavior of azole-based protic ionic liquids: Influence of the alkalinity and physicochemical properties. J. CO_2 Util. 19, 1-8.

Zeng, S.J., Gao, H.S., Zhang, X.C., Dong, H.F., Zhang, X.P., Zhang, S.J., 2014. Efficient and reversible capture of SO_2 by pyridinium-based ionic liquids. Chem. Eng. J. 251, 248-256.

Zeng, S.J., Liu, L., Shang, D.W., Feng, J.P., Dong, H.F., Xu, Q.X., Zhang, X.P., Zhang, S.J., 2018. Efficient and reversible absorption of ammonia by cobalt ionic liquids through Lewis acid-base and cooperative hydrogen bond interactions. Green. Chem. 20(9), 2075-2083.

Zhang, J.Z., Jia, C., Dong, H.F., Wang, J.Q., Zhang, X.P., Zhang, S.J., 2013. A novel

dual amino-functionalized cation-tethered ionic liquid for CO_2 capture. Ind. Eng. Chem. Res. 52(17), 5835-5841.

Zhao, Y., Zhang, X., Zeng, S., Zhou, Q., Dong, H., Tian, X., Zhang, S., 2010. Density, viscosity, and performances of carbon dioxide capture in 16 absorbents of amine plus ionic liquid + H_2O, ionic liquid + H_2O, and amine + H_2O systems. J. Chem. Eng. Data 55(9), 3513-3519.

Zhao, Y., Zhang, X., Zhen, Y., Dong, H., Zhao, G., Zeng, S., Tian, X.,Zhang, S., 2011. Novel alcamines ionic liquids based solvents: Preparation, characterization and applications in carbon dioxide capture. Int. J. Greenh. Gas Con. 5(2), 367-373.

Zhu, X., Song, M.L.,Xu, Y.J., 2017. DBU-based protic ionic liquids for CO_2 capture. ACS Sustain. Chem. Eng. 5(9), 8192-8198.

Supporting Information

Protic ionic liquids with low viscosity for efficient and reversible capture of carbon dioxide

Fangfang Li[a,b], Yinge Bai[a], Shaojuan Zeng[a,**], Xiaodong Liang[c], Hui Wang[a], Feng Huo[a], Xiangping Zhang[a,b,*]

[a] Beijing Key Laboratory of Ionic Liquids Clean Process, CAS Key Laboratory of Green Process and Engineering, State Key Laboratory of Multiphase Complex Systems, Institute of Process Engineering, Chinese Academy of Sciences, Beijing 100190, China

[b] Sino-Danish College of University of Chinese Academy of Sciences, Beijing 100049, China

[c] Department of Chemical and Biochemical Engineering, Technical University of Denmark, DK-2800 Lyngby, Denmark

* Corresponding author. E-mail: xpzhang@ipe.ac.cn, Tel/Fex: 86-10-8254-4875

** Corresponding author. E-mail: sjzeng@ipe.ac.cn

FTIR data of all studied ionic liquids
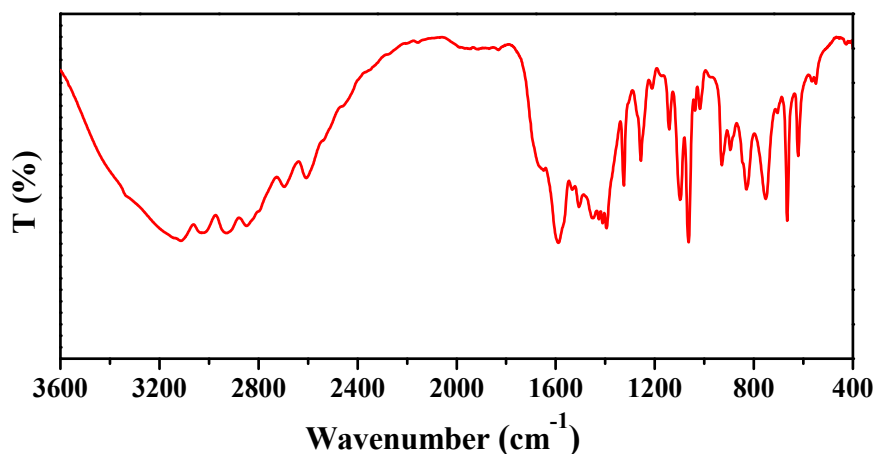
Fig. S1. FTIR spectra of [TMGH][Im]

υ =2925.51 (the stretching vibration of CH$_3$), 2696.10 (the characteristic peak of N-CH$_3$), 1589.07 (the stretching vibration of C=N), 1506.18 and 1410.72 (the stretching vibration of imidazole ring skeleton), 1063.47 cm^{-1} (the stretching vibration of C-N).
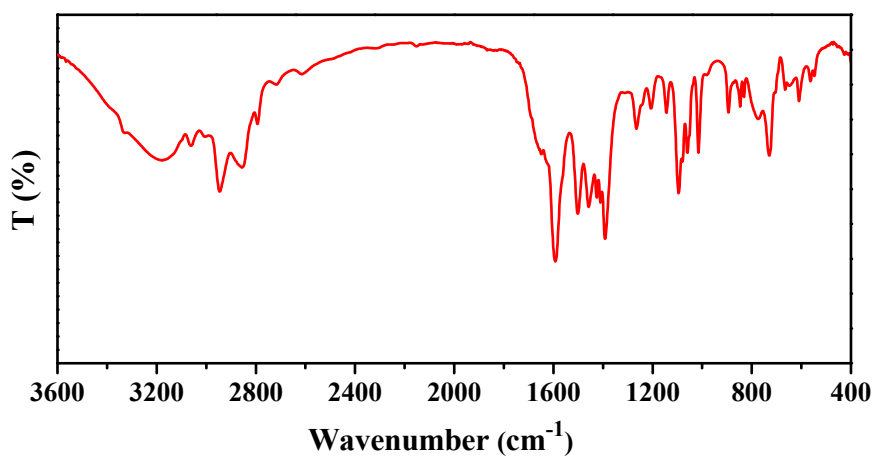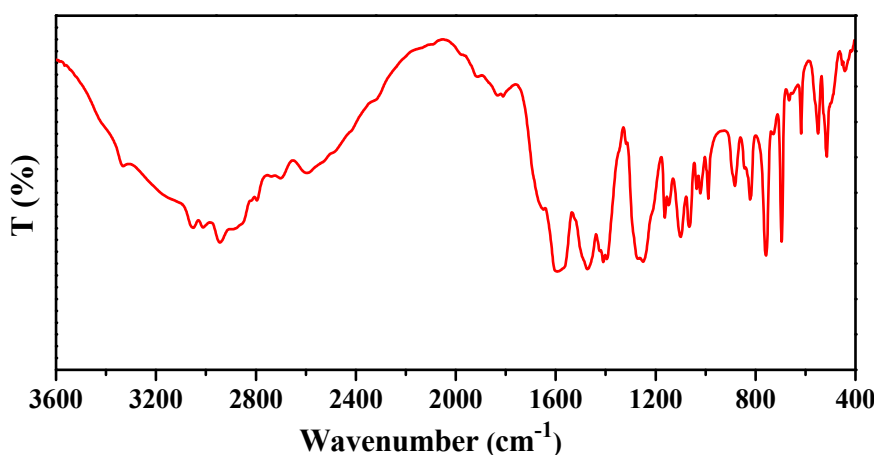

Fig. S2. FTIR spectra of [TMGH][Pyrr]

υ =2945.69 (the stretching vibration of CH$_3$), 1592.28 (the stretching vibration of C=N), 1501.53 and 1457.70 (the stretching vibration of pyrrole ring skeleton), 1095.02 cm^{-1} (the stretching vibration of C-N).

Fig. S3. FTIR spectra of [TMGH][PhO]

υ =2943.95 (the stretching vibration of CH_3), 2595.64 (the characteristic peak of N-CH_3), 1593.44 (the stretching vibration of C=N), 1472.91 and 1409.27 (the stretching vibration of imidazole ring skeleton), 1250.10 (the stretching vibration of C-O), 1099.71 cm^{-1} (the stretching vibration of C-N).
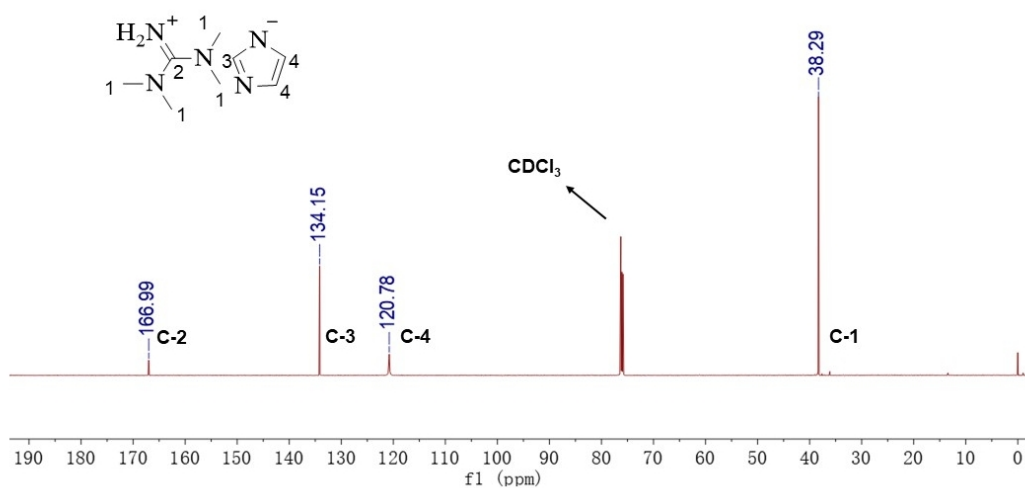
^{1}H NMR and ^{13}C NMR data of all studied ionic liquids
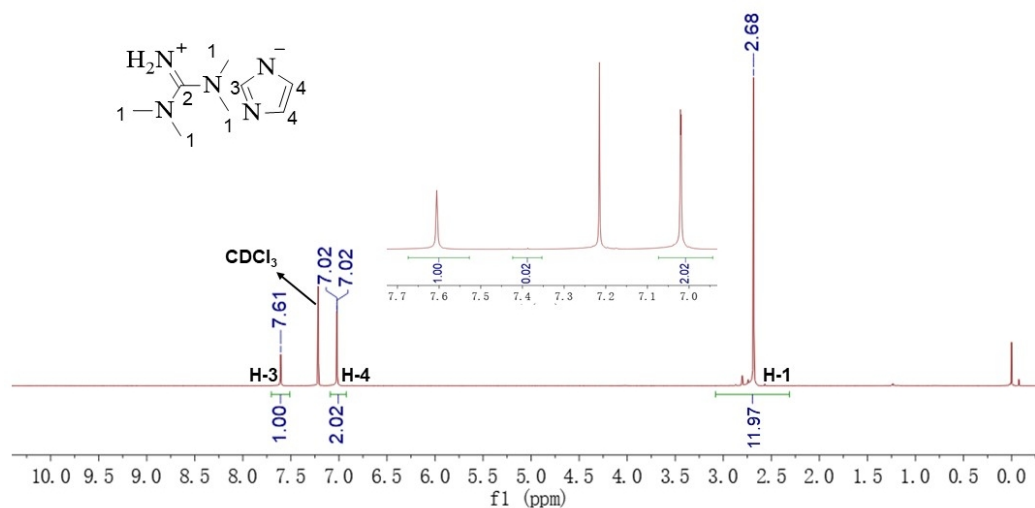
Fig. S4. ^{1}H NMR spectra of [TMGH][Im]

^{1}H NMR (600 MHz; $CDCl_3$; TMS): 2.68 (12H, s, CH_3), 7.02 (2H, s, CH), 7.61 ppm (1H, s, CH).

The purity of [TMGH][Im] was estimated by comparing area of the CH-3 signal with its signal area between δ 7.35 and 7.38, the obtained purity is 0.98.
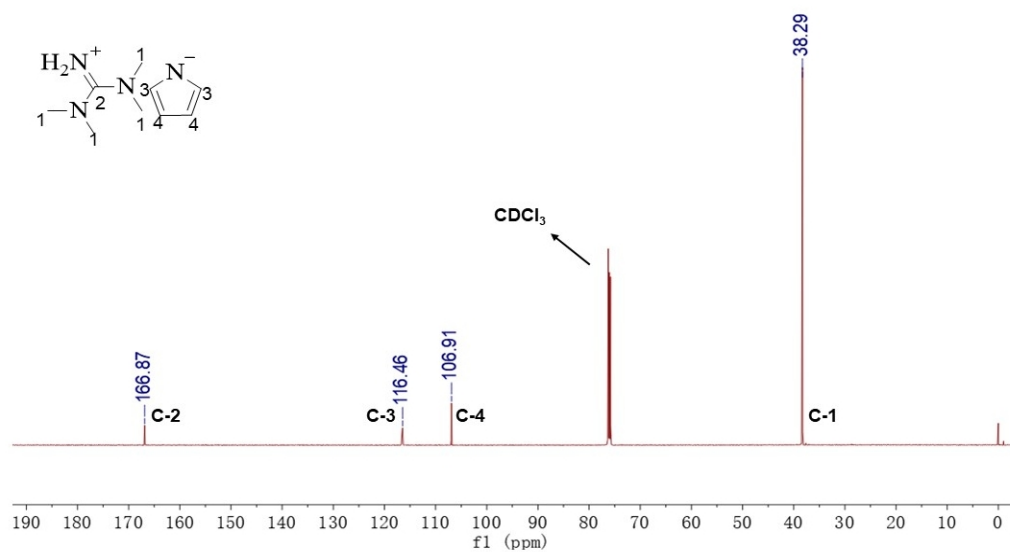
Fig. S5. ^{13}C NMR spectra of [TMGH][Im]

^{13}C NMR (600 MHz; CDCl$_3$; TMS): 38.29, 120.78, 134.15, 166.99 ppm.
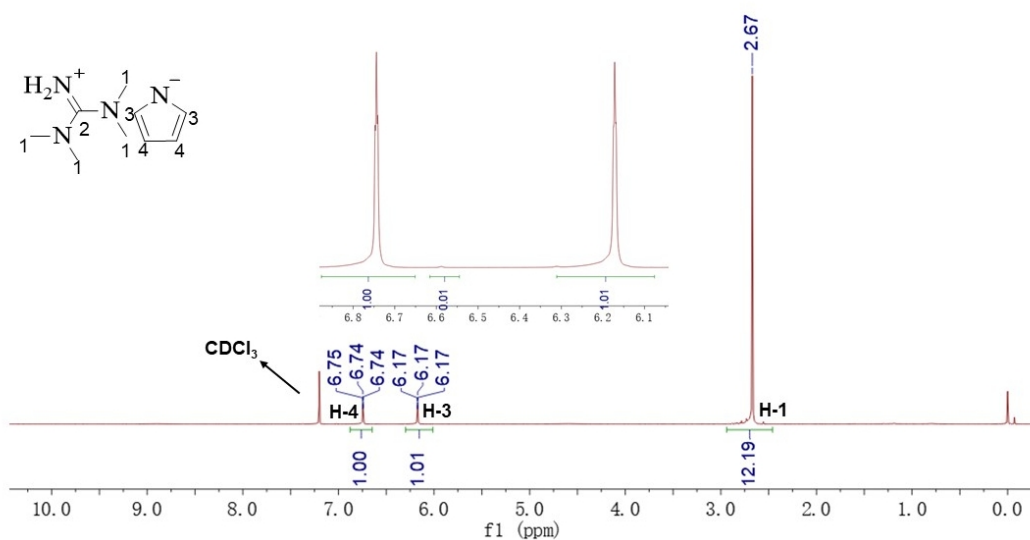
Fig. S6. ^{1}H NMR spectra of [TMGH][Pyrr]
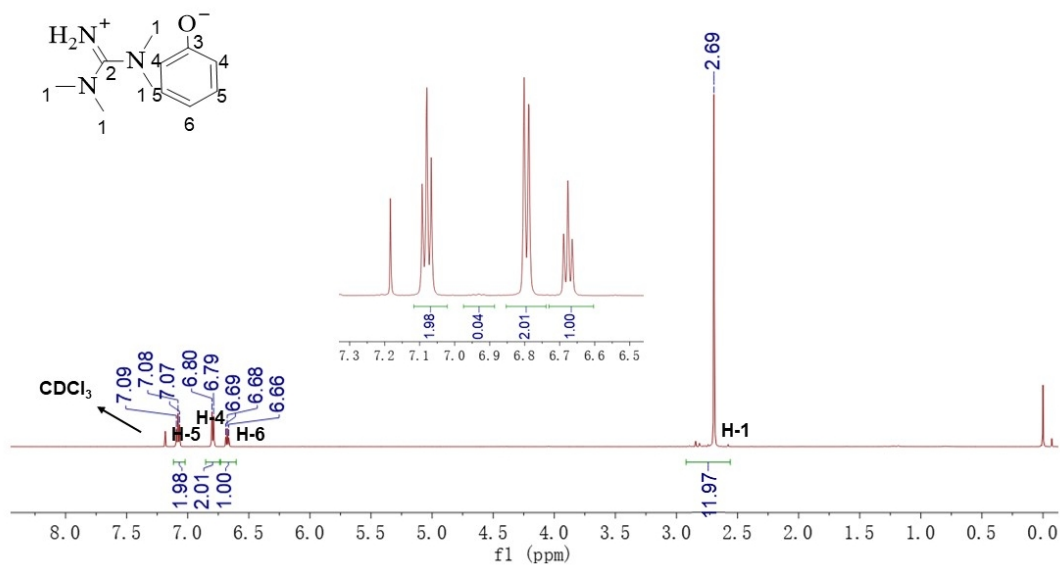
^{1}H NMR (600 MHz; CDCl$_3$; TMS): 2.67 (12H, s, CH$_3$), 6.17 (2H, d, CH), 6.74 ppm (2H, d, CH).

The purity of [TMGH][Im] was estimated by comparing area of the CH-4 signal with its signal area between δ 6.55 and 6.61, the obtained purity is 0.99.
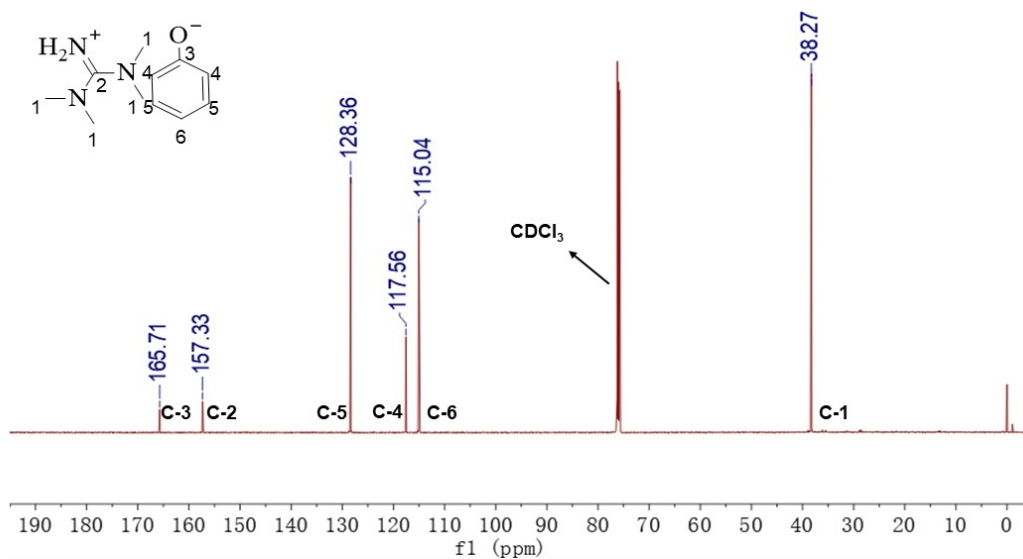
Fig. S7. ^{13}C NMR spectra of [TMGH][Pyrr]

^{13}C NMR (600 MHz; CDCl$_3$; TMS): 38.29, 106.91, 116.46, 166.87 ppm.

Fig. S8. ^{1}H NMR spectra of [TMGH][PhO]

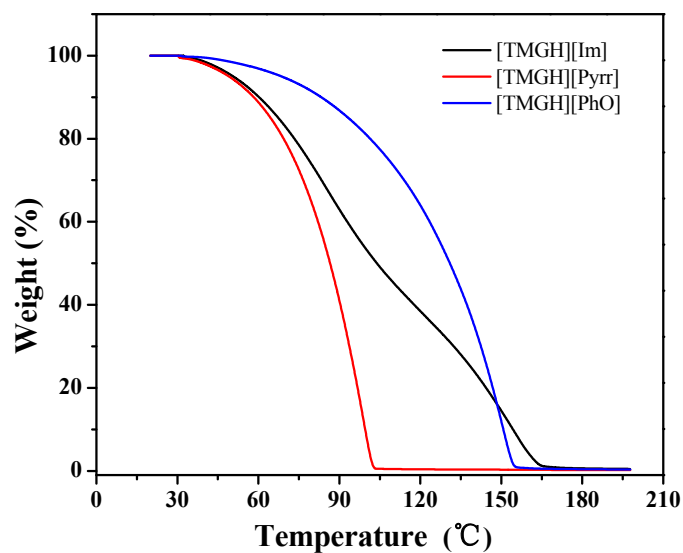^{1}H NMR (600 MHz; CDCl$_3$; TMS): 2.69 (12H, s, CH$_3$), 6.68 (H, t, CH), 6.79 (2H, d, CH), 7.08 ppm (2H, t, CH).

The purity of [TMGH][Im] was estimated by comparing area of the CH-5 signal with its signal area between δ 6.89 and 6.96, the obtained purity is 0.98.

Fig. S9. ^{13}C NMR spectra of [TMGH][PhO]

^{13}C NMR (600 MHz; CDCl$_3$; TMS): 38.27, 115.04, 117.56, 128.36, 157.33, 165.71ppm.

TGA of all studied ionic liquids

Fig. S10. TGA of [TMGH][Im]、[TMGH][Pyrr] and [TMGH][PhO]